(III) the donor centers are deep in the forbidden gap but are so concentrated that wave functions overlap and "impurity band" conduction results. In the case of alkali-doped transition metal oxides, models I and III appear to be excluded—model I, because it predicts metallic behavior at all concentrations of donor centers (whereas low concentrations of M or of oxygen defect in WO_3 result in semiconductivity), and model III, because it predicts that the conduction band wave functions should have substantial donor atomic orbital character (whereas nmr studies suggest such contributions are negligible). Model II thus appears the most suitable; it can be visualized as resulting from a cooperative ionization of all of the donor centers because of mutual screening by all of the delocalized electrons against recapture of electrons by the ionized donor centers.

However, it may not be so easy to distinguish models I, II, and III as the above implies. In Li_xWO_3, for example, it has been suggested[5] that the donor center is not simply the Li atom in the host WO_3 matrix but rather the cage of tungsten atoms around the Li^+ to which the electron has been transferred. Such a transfer complicates matters enormously because the impurity level (Li^0) is definitely above the conduction band, the actual donor center (Li^+-centered tungsten cage with associated electron) is below the band, and, most important of all, the orbitals contributing to the conduction band (nonperturbed W atoms) are very similar to the orbitals describing the localized electron (perturbed W atoms). With increasing impurity concentration, the onset of metallic behavior can be described equally well as resulting from overlap of the actual donor centers or from cooperative ionization of the donor centers into a host conduction band.

In $Ta_{2+x}O_5$, the tantalum interstitials may themselves be the donor centers, in which case model I would require them to lie above the Ta_2O_5 conduction band whereas model II would place them just below the conduction band but at such high concentration that degenerate electron behavior results. Model III would appear to be unsuitable for this material since the spacing between Ta interstitials is greater than between Ta interstitials and Ta normal sites. Models I and II could be distinguished by studying the behavior at low concentration of Ta interstitials. (We tried to do this but found that the material could not be synthesized with less than a large concentration of interstitials.) At low concentration of interstitials, model I would predict zero activation energy for electron transport, and model II would predict finite activation energy provided the concentration of interstitials was low enough. An alternate picture is that the Ta interstitials are not the donor centers but have transferred their electrons to other structural features (*e.g.*, dislocations) which then act as donor centers. In such case, metallic behavior could also result if the donor density were high enough to produce degenerate behavior.

Contribution No. 66-34 from the College of Earth and Mineral Sciences,
The Pennsylvania State University, University Park, Pennsylvania 16802

Phase Relationships in the System $SrO–P_2O_5$ and the Influence of Water Vapor on the Formation of $Sr_4P_2O_9$

By Eric R. Kreidler and F. A. Hummel

Received October 21, 1966

Phase relationships in the system $SrO–P_2O_5$ were determined by quenching, strip furnace, vacuum heat treatment, and high-temperature X-ray diffraction methods. The results of experiments done in air at temperatures below 1400° on compositions near the SrO end of the system can be interpreted only by considering water vapor as a component of the system. The data were used to construct phase diagrams for the system $SrO–P_2O_5$ and a portion of the system $SrO–P_2O_5–H_2O$. The melting behavior and polymorphism of the six binary compounds is discussed in detail. The $SrO–P_2O_5$ system is compared with the previously reported $CaO–P_2O_5$ system. Limited data for the $CaO–P_2O_5$ system indicate errors in the reported diagrams, and a new diagram for the $CaO–P_2O_5$ system is proposed, but it is emphasized that a careful reinvestigation of this system is needed.

Introduction and Literature Survey

The $SrO–P_2O_5$ system is of technological importance because two of the compounds in the system, $Sr_2P_2O_7$ and $Sr_3(PO_4)_2$, serve as host structures for efficient tin-activated (Sn^{2+}) phosphors.

Although no phase diagram has been published for the $SrO–P_2O_5$ system, Ropp, Aia, Hoffman, Veleker, and Mooney[1] have published very reliable X-ray diffraction patterns for most of the anhydrous compounds and their polymorphs. The phases reported were: γ-, β-, and α-strontium metaphosphate, $Sr(PO_3)_2$; β- and α-strontium pyrophosphate, $Sr_2P_2O_7$; strontium orthophosphate, $Sr_3(PO_4)_2$; and strontium hydroxylapatite, $Sr_{10}(PO_4)_6(OH)_2$. The phase transitions were studied by differential thermal analysis and thermogravimetric analysis. The following transition points were found

---

[1] R. C. Ropp, M. A. Aia, C. W. W. Hoffman, T. J. Veleker, and R. W. Mooney, *Anal. Chem.*, **31**, 1163 (1959).

$$\gamma\text{-Sr(PO}_3)_2 \xrightarrow{420^\circ} \beta\text{-Sr(PO}_3)_2 \xrightarrow{850^\circ} \alpha\text{-Sr(PO}_3)_2 \xrightarrow{980^\circ} \text{liquid} \quad \text{(a)}$$

$$\beta\text{-Sr}_2\text{P}_2\text{O}_7 \xrightarrow{760^\circ} \alpha\text{-Sr}_2\text{P}_2\text{O}_7 \quad \text{(b)}$$

The reversibility of these reactions was not discussed. Except for $Sr_3(PO_4)_2$, all of the anhydrous crystalline phases were prepared by heat treating various precipitated products. Strontium orthophosphate was prepared by allowing mixtures of $SrCO_3$ and $Sr_2P_2O_7$ to react in the solid state. In addition to the anhydrous phases, X-ray diffraction patterns were reported for six hydrated strontium phosphates.

Sarver, Hoffman, and Hummel[2] found by high-temperature X-ray diffraction analysis that $Sr_3(PO_4)_2$ undergoes a rapid reversible phase transition at 1305°. The high-temperature form, β-$Sr_3(PO_4)_2$, is isotypic with whitlockite, β-$Ca_3(PO_4)_2$, and although pure β-$Sr_3(PO_4)_2$ cannot be quenched to room temperature, it forms solid solutions of the type $(Sr_{1-x}M_x)_3(PO_4)_2$ (where $x \sim 0.15$ and M = Ca, Mg, or Zn) which can be cooled to room temperature while retaining the β structure. The low-temperature or α form is the same as that observed by Ropp, *et al.*[1] Zachariasen[3] has determined the structure of α-$Sr_3(PO_4)_2$.

McKeag and Steward[4] prepared strontium tetraphosphate, $Sr_3P_4O_{13}$, by solid-state reaction and published its X-ray diffraction pattern. At high temperatures strontium tetraphosphate loses P_2O_5 by vaporization thereby causing the composition and crystal structure to revert to those of the pyrophosphate.

The compound $Sr_4P_2O_9$ was reported by Bauer and Balz,[5] who found it to be isostructural with the analogous calcium compound $Ca_4P_2O_9$. Bauer and Balz found that $Sr_4P_2O_9$ is orthorhombic, having space group P222$_1$. According to Brown and Epstein,[6] $Ca_4P_2O_9$ is in fact monoclinic, having four formula units per unit cell and space group P2$_1$. A comparison of the lattice parameters for these two compounds is given in Table I.[5-7] From this comparison it may be seen that the monoclinic cell reported by Brown and Epstein is only slightly distorted from an orthorhombic cell. In view of the close similarity between the axial ratios (a/c and b/c), the two compounds are probably isostructural as reported by Bauer and Balz.

Balz[8] has also reported the existence of strontium oxyapatite, $Sr_{10}(PO_4)_6O$. The existence of the oxyapatites has been a controversial subject for some time. However, since the work of Wondratschek[9] on lead oxyapatite, the case for the existence of the oxyapatites has become considerably stronger. Balz, in particular, has found that the oxyapatites, $A_{10}(XO_4)_6O$, appear to exist only when the radius ratio r_X/r_A is less than 0.30 (Ahrens radii). Calcium does not fit this requirement, and no calcium oxyapatite exists. On the other hand, Sr, Pb, and Ba do fit the requirement and oxyapatites of each of these have been reported.

TABLE I

	$Ca_4P_2O_9$[6] (monoclinic)	$Sr_4P_2O_9$[5,7] (orthorhombic)
a, A	11.99	12.57
b, A	9.48	9.79
c, A	6.97	7.38
α, deg	90.8	90
β, deg	90	90
γ, deg	90	90
a/c	1.72	1.70
b/c	1.36	1.33

In view of the similarity of the ionic radii of Ca^{2+} (0.99 A) and Sr^{2+} (1.12 A) the CaO–P_2O_5 and SrO–P_2O_5 systems should be quite similar. A number of investigations on the CaO–P_2O_5 system have been published and these results were used as a guide in the present study. One of the earlier studies was by Tromel, Harkort, and Hotop in 1948.[10] These authors studied the part of the system extending from 20 to 100 wt % CaO. Four compounds were found: $Ca(PO_3)_2$, $Ca_2P_2O_7$ having an inversion $\beta \rightarrow \alpha$ at about 1130°, $Ca_3(PO_4)_2$ having an inversion $\beta \rightarrow \alpha$ at about 1200°, and $Ca_4P_2O_9$. The first three compounds melted congruently at 980, 1300, and 1730°, respectively, while $Ca_4P_2O_9$ melted incongruently at 1630°. In 1961, Welch and Gutt[11] published a new diagram covering the portion of the system from 43 to 65 wt % CaO. Aside from relatively minor differences in the reported melting points, the new diagram shows a rather extensive solid solution series (50–54 wt % CaO or 71.7–75 mole % CaO) which was not observed by Tromel, *et al.* There are very strong experimental reasons for suspecting that this solid solution series does not exist (see Results and Discussion section). It should be noted that Welch and Gutt gave no direct evidence such as lattice parameter or refractive index changes which would prove the existence of these solutions. Furthermore the experimental technique employed in their study (high-temperature microscopy) may yield erroneous results. Welch and Gutt reported a third polymorph of calcium orthophosphate, α'-$Ca_3(PO_4)_2$, which exists above 1430° and is nonquenchable.

Hill, Faust, and Reynolds[12] in 1944 studied the portion of the system extending from 0 to 44 wt % CaO by the quenching technique. Water was excluded from the system by preparing samples in a dry chamber and heating them in sealed glass tubes.

Two ultraphosphate compounds were reported. These were CaP_4O_{11} which melted congruently at 800° and $Ca_2P_6O_{17}$ which melted incongruently at 770°.

Calcium metaphosphate was found to have a quench-

---

(2) J. F. Sarver, M. V. Hoffman, and F. A. Hummel, *J. Electrochem. Soc.*, **108**, 1103 (1961).

(3) W. H. Zachariasen, *Acta Cryst.*, **1**, 263 (1948).

(4) A. H. McKeag and E. G. Steward, *British J. Appl. Phys.*, **4**, S26 (1955).

(5) H. Bauer and W. Balz, *Z. Anorg. Allgem. Chem.*, **340**, 225 (1965).

(6) W. E. Brown and E. F. Epstein, *J. Res. Natl. Bur. Std.*, **69**, 547 (1965).

(7) The values of a and c given by Bauer and Balz have been interchanged for the comparison. This is permissible since the naming of orthorhombic axes is arbitrary.

(8) W. Balz, Dissertation, T. H. Karlsruhe, 1961. Findings discussed by H. Wondratschek.[9]

(9) H. Wondratschek, *Neues Jahrb. Mineral. Abhandl.*, **99**, 113 (1963).

(10) G. Tromel, H. J. Harkort, and W. Hotop, *Z. Anorg. Chem.* **256**, 253 (1948).

(11) J. H. Welch and W. Gutt, *J. Chem. Soc.*, 4442 (1961).

(12) W. L. Hill, G. T. Faust, and D. S. Reynolds, *Am. J. Sci.*, **242**, 457, 542 (1944).

able high-temperature form, α-$Ca(PO_3)_2$, which was stable above 963°. Extensive solid solutions of $Ca_2P_2O_7$ in β-$Ca(PO_3)_2$ (28.3–34.0 wt % CaO) and $Ca(PO_3)_2$ in β-$Ca_2P_2O_7$ (41–44 wt % CaO) were reported. A slight but consistent change in refractive index was reported for the β-$Ca(PO_3)_2$ solid solutions. In addition, an intermediate solid solution series, named trömelite, was reported. These solid solutions are centered about the molar ratio 7CaO:$5P_2O_5$, melt incongruently at 985° to β-$Ca_2P_2O_7$(ss) + liquid, and have a lower limit of stability at 920°.

Experimental Procedures

The compositions studied[13] were prepared by allowing chemically pure $SrCO_3$ and $(NH_4)_2HPO_4$ to react in the solid state. The starting materials were thoroughly mixed under acetone and then heated in Pt crucibles to temperatures of 500, 750, and 920°[14] with intermediate mixing under acetone. These materials were used as the starting materials in the quench and strip furnace studies.

The phases present in each sample were identified by means of the petrographic microscope (particularly when glass was present) or by means of X-ray diffraction analysis. For routine phase analysis, the Norelco diffractometer was set at a scanning rate of 2° (2θ)/min. When more accurate measurements were required, the scanning rate was set at 0.25° (2θ)/min. In both cases the chart speed was 1 in./min. All patterns were taken with Ni-filtered copper radiation. High-temperature X-ray diffraction patterns were made with a Tem-Pres type of furnace mounted on the Norelco diffractometer.

Several methods of heat treatment were used. The quenchable solid $\rightleftarrows$ solid and solid $\rightleftarrows$ liquid reactions were studied by the conventional quenching technique. The melting behavior of the SrO–$Sr_2P_2O_7$ portion of the system was studied with a strip furnace. Essentially this apparatus consists of a variable-power supply, a V-shaped Pt or Pt–40Rh strip, and an optical pyrometer. The temperature of the platinum strip could be accurately controlled by a fine adjustment on the power supply. Melting points were determined by placing a small amount of sample ($\approx$0.3 mg) on the strip and observing when melting first occurred as the power was slowly increased. The temperature was immediately read with a Leeds and Northrup pyrometer which had been calibrated against the melting points of diopside (1391°) and 10% MgO–90% SiO_2 (1695°). The pyrometer also served as a low-power telescope to observe when melting occurred. The condition of each sample was rechecked with a binocular microscope to ensure that melting had occurred. The melting points determined in this way were reproducible within 20°, and those listed in Table I are the average of at least three determinations.

A limited number of heat treatments were made under vacuum in an attempt to eliminate water from the system. These heat treatments were made by packing the samples into $^1/_8$-in. platinum tubes open at one end. A number of these platinum tubes were placed into a silica tube sealed at one end. A vacuum pump was connected to the open end of the silica tube and started; then the entire assembly was lowered into a quench furnace. The vacuum was maintained until the samples had been cooled to room temperature after completion of the heat treatment. The results of the experiments done under vacuum were compared with the results of the same experiments done in air (Table II).

All other heat treatments were done in a conventional Globar furnace. The samples were either pressed into $^1/_2 \times ^1/_8$ in. pellets and heated on a platinum sheet or tamped into platinum crucibles.

Results and Discussion

The System SrO–P_2O_5

Several problems were encountered in working out the phase equilibrium diagram for the system SrO–P_2O_5 (Figure 1). From 0 to 25 mole % P_2O_5, it is very difficult to completely exclude water from the system, and in order to interpret the results of experiments done in air at temperatures below 1400° it is necessary to consider the ternary system SrO–P_2O_5–H_2O. A discussion of these effects is given in a later section. Samples containing between 60 and 100 mole % P_2O_5 formed low-melting glasses which were rapidly attacked by water vapor at room temperature. The liquidus temperature at 60 mole % P_2O_5 was less than 550°. In view of the difficulty of excluding water from the high phosphate compositions[12] and the difficulty of obtaining equilibrium at such low temperatures, it was felt that further investigation of the portion of the system from 60 to 100 mole % P_2O_5 was unwarranted.

The glass-forming region in this system extends from about 40 to 100 mole % P_2O_5. The solidus lines in the system are known accurately, but no attempt was made to determine accurately eutectic compositions or points on the liquidus curve. The general configuration of the liquidus curve as shown in Figure 1 is believed to be correct.

Six compounds exist in the system. In order of increasing P_2O_5 content these are: $Sr_4P_2O_9$ (tetrastrontium phosphate), $Sr_{10}(PO_4)_6O$ (strontium oxyapatite), $Sr_3(PO_4)_2$ (strontium orthophosphate), $Sr_2P_2O_7$ (strontium pyrophosphate), $Sr_3P_4O_{13}$ (strontium tetraphosphate), and $Sr(PO_3)_2$ (strontium metaphosphate). All of these compounds have been previously reported.[1,4,5,8]

Tetrastrontium phosphate melted incongruently at 1560° to SrO plus liquid. This behavior was identical with that of the calcium analog, $Ca_4P_2O_9$.[11] Tetrastrontium phosphate cannot be synthesized in air at temperatures below 1400°. This is due to the interference of water vapor which favors the formation of a mixture of strontium hydroxylapatite and strontium oxide. The compound can be synthesized by heating the stoichiometric mixture of $Sr_3(PO_4)_2$ and $SrCO_3$ under vacuum at 1400°, or by melting samples at 1650° on the strip furnace. No polymorphism was observed in $Sr_4P_2O_9$. The X-ray diffraction pattern of $Sr_4P_2O_9$ is given in Table III.

Strontium oxyapatite melted congruently at about 1600°, and no evidence of polymorphism was found. When synthesized in air at temperatures below 1400°, the compound present is actually strontium hydroxylapatite, $Sr_{10}(PO_4)_6(OH)_2$. The X-ray diffractometer patterns of the hydroxylapatite and oxyapatite are identical and additional evidence is necessary to establish the existence of the oxyapatite. This evidence is given in the section dealing with phase equilibria in a portion of the system SrO–P_2O_5–H_2O.

---

[13] Pertinent data have been deposited as Document No. 9294 with the ADI Auxiliary Publications Project, Photoduplication Service, Library of Congress, Washington 25, D. C. A copy may be secured by citing the document number and by remitting $1.25 for photoprints, or $1.25 for 35-mm microfilm. Advance payment is required. Make checks or money orders payable to: Chief, Photoduplication Service, Library of Congress.

[14] Except for samples richer in P_2O_5 than $Sr(PO_3)_2$ which were heated only to 550°.

TABLE II

EQUILIBRIUM DATA FOR THE SYSTEM $SrO-P_2O_5-H_2O$

Heat treatment, deg/hr	Remarks	Composition, mole % P_2O_5 — 10.0	16.6	20.0^b	21.4	23.0	24.0
		Phases present[a]					
				($Sr_4P_2O_9$)		($Sr_{10}(PO_4)_6O$)[b]	
1014/19	In air	SrO + Ap·	...	Ap·	Ap·	Ap· + α-S_3P	α-S_3P + Ap·
1240/11	In air	...	Ap· + tr·SrO	Ap· + tr·SrO + tr·S_4P	Ap· + tr·SrO	Ap· + α-S_3P	α-S_3P + Ap·
1450/3	In air	...	Ap· + S_4P + SrO	Ap· + S_4P + SrO	Ap· + S_4P	Ap· + α-S_3P	α-S_3P + Ap·
1420/2	Vacuum	...	S_4P + tr·SrO	S_4P + Ap· + SrO	...	Ap· + α-S_3P	α-Sr_3P + Ap·
1650/10 sec.	Fused SF	SrO + S_4P	S_4P + Ap· + SrO	S_4P + Ap·	Ap· + S_4P	Ap· + tr·α-S_3P	α-S_3P + Ap·

[a] Predominant phase listed first. [b] These compositions are slightly richer in P_2O_5 than indicated, which accounts for the appearance of secondary phases.

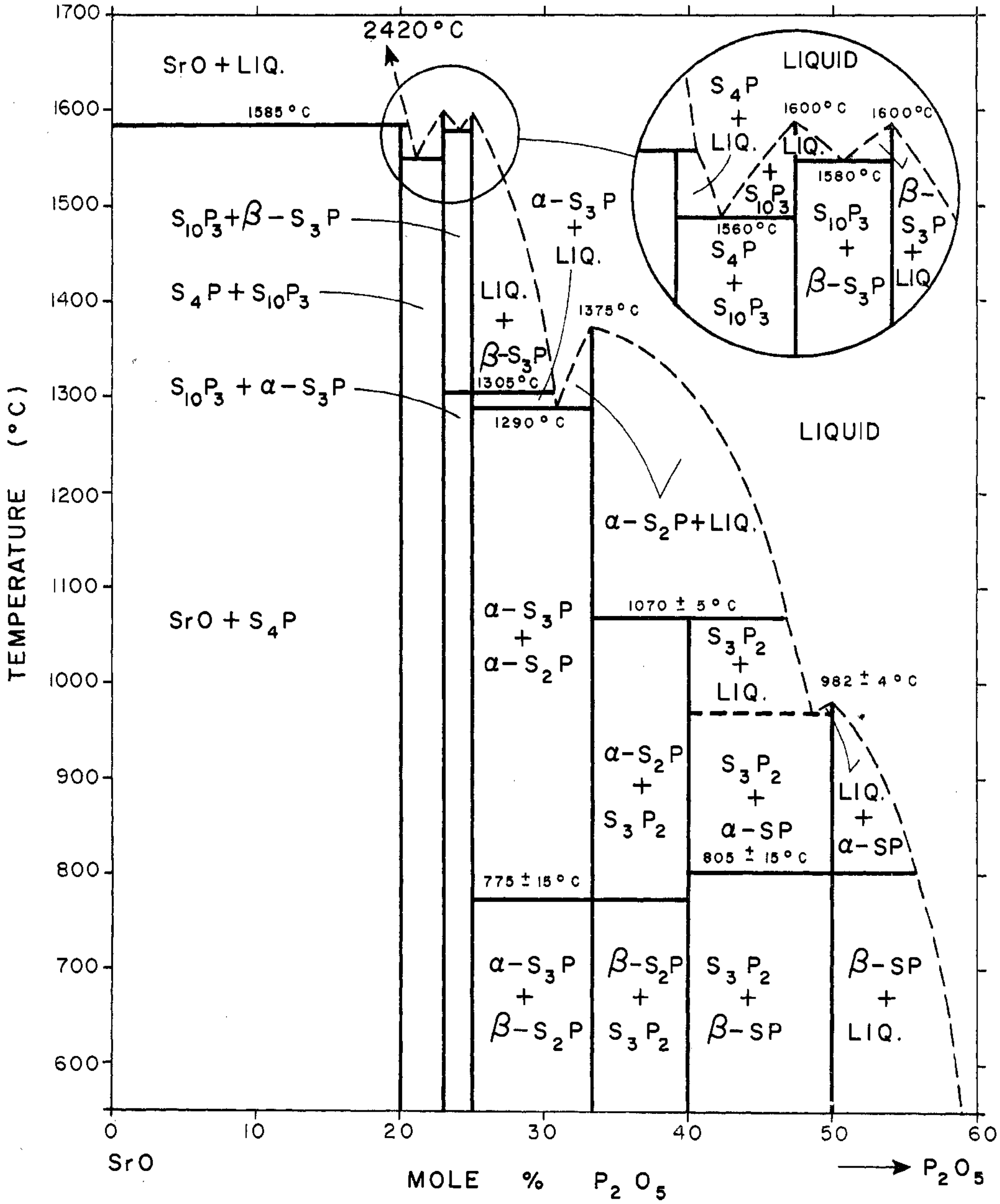

Figure 1.—Phase relations in a portion of the system $SrO-P_2O_5$: S = SrO; P = P_2O_5.

Strontium hydroxylapatite can be dehydrated to give strontium oxyapatite, but the temperature at which complete dehydration occurs is dependent upon the partial pressure of water vapor (P_{H_2O}) in the system. It is likely that a continuous series of solid solutions, having a general formula

$$Sr_{10}(PO_4)_6(OH)_{2-2x}O_x\square_x$$

Table III
X-Ray Diffraction Patterns of $Sr_3P_4O_{13}$ and $Sr_4P_2O_9$

d, A	I/I_1	d, A	I/I_1
		$Sr_3P_4O_{13}$	
7.37	10	2.25	8
4.95	8	2.16	8
4.79	5	2.14	2
4.53	17	2.10	17
3.80	9	2.06	13
3.72	2	2.01	16
3.65	8	1.977	9
3.49	56	1.957	6
3.37	45	1.910	7
3.34	17	1.906	9
3.28	7	1.899	8
3.17	100	1.866	6
3.01	23	1.827	12
2.93	24	1.797	6
2.73	28	1.765	9
2.54	2	1.743	8
2.49	9	1.710	5
2.45	19	1.689	8
2.40	3	1.645	8
2.34	3	1.629	3
2.33	6	1.610	5
2.29	9	1.595	5
2.28	15	+ other reflections	
		$Sr_4P_2O_9$	
4.55	19	2.66	15
4.29	8	2.41	11
4.21	4	2.30	5
3.85	18	2.23	8
3.68	13	2.17	8
3.63	16	2.05	18
3.33	40	2.03	29
3.14	100	1.99	16
3.02	82	1.94	16
2.91	48	1.91	16
2.89	59	1.87	10
2.88	61	1.84	13
2.86	45	1.79	19
2.76	18	+ other reflections	
2.70	8		

where $0 \leq x \leq 1$ and $\square$ = hydroxyl vacancy, exists between oxy- and hydroxylapatite. Strontium oxyapatite was successfully synthesized by heating a mixture of $3Sr_3(PO_4)_2 \cdot SrCO_3$ under vacuum at 1400° or by melting on the strip furnace at 1650°; however, even these samples may have been partially hydrated.

Strontium orthophosphate melted congruently at 1600°. The inversion temperature at 1305° reported by Sarver, Hoffman, and Hummel[2] was accepted as correct, and the high-temperature X-ray diffraction study reported by these authors was not repeated. In agreement with the earlier study, β-$Sr_3(PO_4)_2$ could not be quenched to room temperature.

Strontium pyrophosphate melted congruently at 1375° and could not be quenched to yield a glass. Quenching experiments and high-temperature X-ray diffraction analysis showed that α-$Sr_2P_2O_7$ was stable up to the melting point. The compound has two polymorphs and the low-temperature (β) form inverts to the high-temperature (α) form at 775 ± 15°. The reaction $\beta \rightarrow \alpha$ was sluggish and required more than 2 hr to go to completion when the β form was heated at 814°. Ropp, *et al.*,[1] were just able to detect the inversion by differential thermal analysis and reported that it occurred between 760 and 800°. The reverse reaction ($\alpha \rightarrow \beta$) did not occur when the α form was heated at 675° for 72 hr. β-$Sr_2P_2O_7$ was successfully prepared by dehydrating $SrHPO_4$ at 700°. According to Ropp, *et al.*,[1] the dehydration reaction is complete at 575°.

Strontium tetraphosphate melted incongruently at 1070 ± 5° to liquid plus α-$Sr_2P_2O_7$. When heated at 1000° for long periods of time, the composition shifted toward that of strontium pyrophosphate (due to evaporation of P_2O_5 from the structure) resulting in a mixture of tetra- and pyrophosphate. This phenomenon was also observed by McKeag and Steward.[4] Strontium tetraphosphate is known to exist in only one crystallographic modification. McKeag and Steward[4] published an X-ray diffraction pattern for a sample of $Sr_3P_4O_{13}$ containing 2% tin. A more complete pattern for the pure material is given in Table III.

Ropp, Aia, Hoffman, Veleker, and Mooney[1] reported the following reactions for strontium metaphosphate

$$SrH_2P_2O_7 \longrightarrow \gamma\text{-}Sr(PO_3)_2 \qquad 320° \qquad (1)$$

$$\gamma \longrightarrow \beta \qquad 420° \qquad (2)$$

$$\beta \longrightarrow \alpha \qquad 850° \qquad (3)$$

$$\alpha \longrightarrow \text{liquid} \qquad 980° \qquad (4)$$

Only two of these forms (β and α) were found in the present study, but no work was done on the hydrated salts. The γ form of $Sr(PO_3)_2$ is similar to the β form of $Sr_2P_2O_7$ in that neither can be synthesized by the solid-state reaction of $SrCO_3$ with $(NH_4)_2HPO_4$, nor can these be prepared by reheating the high-temperature polymorphs below the inversion points. The $\beta \rightleftarrows \alpha$ inversion temperature as determined by quenching was 805 ± 15° and not 850° as reported by Ropp, *et al.* The inversion is sluggish, and the process $\alpha \rightleftarrows \beta$ was not complete after heating the α form for 37 hr at 790°. The reverse process ($\beta \rightarrow \alpha$) proceeded at a faster rate, but was still incomplete after heating the β form at 826° for 21 hr. Ropp, *et al.*, determined the $\beta \rightleftarrows \alpha$ inversion temperature by differential thermal analysis, a technique which is accurate only for rapid processes. The congruent melting point was determined by quenching to be 982 ± 4°. The value agrees with the previously reported[1] melting point of 980°.

The existence of solid solutions in the system SrO–P_2O_5 was carefully checked by equilibrating pressed pellets of selected compositions and then accurately measuring the position of the X-ray diffraction peak of the phases present. The data given in Table IV prove conclusively that the peak positions of all phases checked are constant within experimental error and independent of sample composition. The fact that no solid solutions occur in the SrO–P_2O_5 system raises serious doubts about the existence of the solid solutions reported in the analogous CaO–P_2O_5 system.[11,12]

TABLE IV

ACCURATE 2θ MEASUREMENTS OF PHASES IN THE SYSTEM $SrO-P_2O_5$ AS A CHECK FOR SOLID SOLUTIONS

$Sr(PO_3)_2$	$Sr(PO_3)_2$ + $Sr_3P_4O_{13}$	$Sr_3P_4O_{13}$	
43.42 ± 0.01	43.42 ± 0.01	...	Equilibrated at 960° for 20 hr
47.14	47.14	...	
56.58	56.57	...	
...	33.64	33.64 ± 0.01	
...	42.98	43.01	
...	44.93	44.93	

$Sr_3P_4O_{13}$	$Sr_3P_4O_{13}$ + $Sr_2P_2O_7$	$Sr_2P_2O_7$	
30.39 ± 0.01	30.38 ± 0.01	...	Equilibrated at 960° for 20 hr
36.48	36.48	...	
43.01	42.99	...	
...	48.84	48.85 ± 0.01	
...	49.28	49.28	
...	55.13	55.14	

$Sr_2P_2O_7$	$Sr_2P_2O_7$ + $Sr_3(PO_4)_2$	$Sr_3(PO_4)_2$	
44.34 ± 0.01	44.34 ± 0.01	...	Equilibrated at 1250° for 20 hr
48.85	48.87	...	
49.29	49.33	...	
...	69.77	69.77 ± 0.01	
...	71.64	71.64	
...	77.57	77.56	

Phase Equilibria in the System $SrO-P_2O_5-H_2O$

As has been previously mentioned, the results of experiments done in air at temperatures below 1400° on samples containing 0–25 mole % P_2O_5 can be interpreted only by considering the effect of water vapor. The results of experiments on several compositions are given in Table II. Two facts should be noted: (a) when fired in air at low temperatures all compositions richer in SrO than $Sr_{10}(PO_4)_6O$ give mixtures of apatite and strontium oxide, but at higher temperatures or when fired under vacuum, these samples contain $Sr_4P_2O_9$; (b) the supposedly binary compositions frequently give mixtures of the three phases $Sr_{10}(PO_4)_6(OH)_2$, $Sr_4P_2O_9$, and SrO when heated at high temperatures. This phase assemblage would be impossible in the binary system $SrO-P_2O_5$. These phenomena can be explained with the aid of Figure 2, which represents the phase relationships in a portion of the system $SrO-P_2O_5-H_2O$. In Figure 2 it has been assumed that a series of solid solutions exists between strontium hydroxylapatite and strontium oxyapatite having the general formula

$$Sr_{10}(PO_4)_6(OH)_{2-2x}O_x\square_x$$

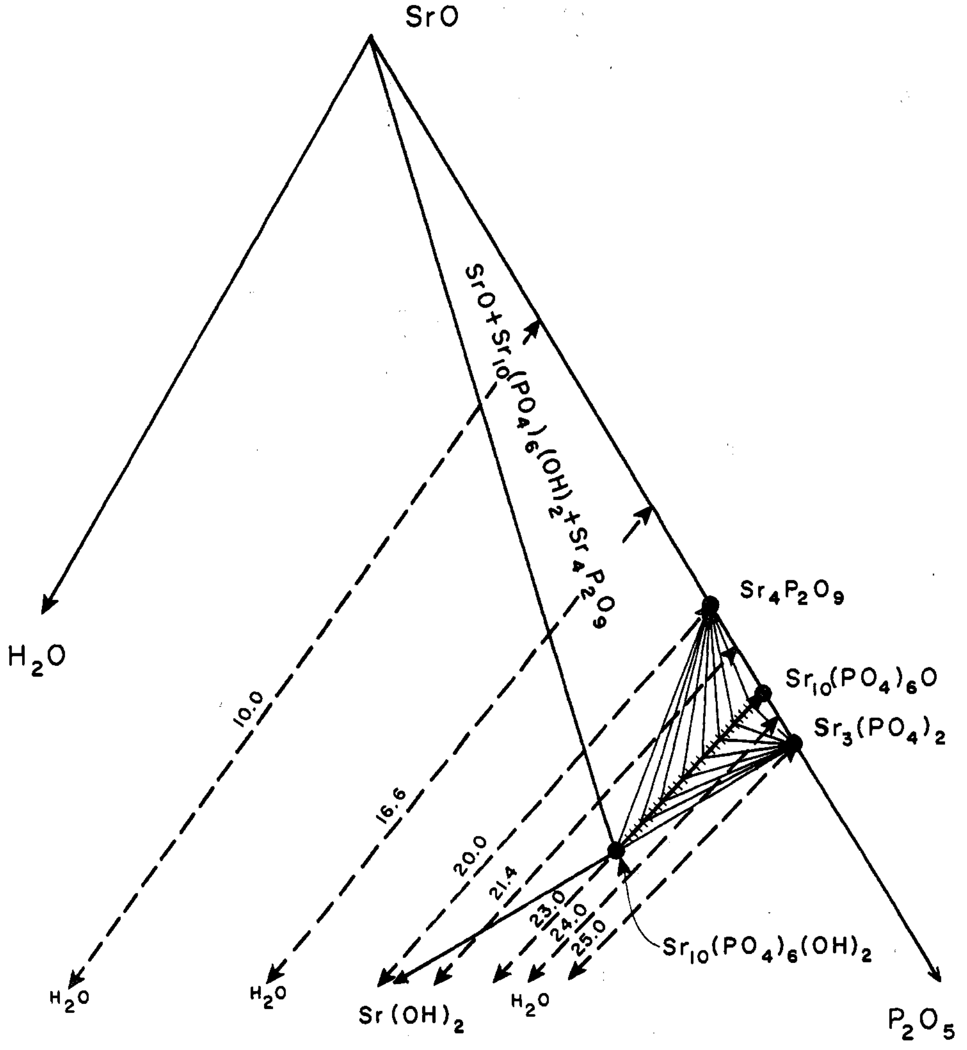

Figure 2.—Phase relations in the system $SrO-P_2O_5-H_2O$ in the neighborhood of strontium hydroxylapatite. The numbers correspond to the compositions listed in Table II.

where $0 \leq x \leq 1$ and $\square$ = a hydroxyl vacancy. The apatite solid solutions would result in two two-phase regions [$Sr_3(PO_4)_2$ + apatite solid solutions] and [$Sr_4P_2O_9$ + apatite solid solutions]. In addition, the diagram would contain the three-phase region [$SrO + Sr_4P_2O_9 + Sr_{10}(PO_4)_6(OH)_2$]. The solid lines in Figure 2 represent the binary joins, and the dashed lines intersect the H_2O apex and represent the paths followed by compositions having fixed $SrO:P_2O_5$ ratios as water is added or subtracted from the system. The actual water content of a sample depends upon the temperature and partial pressure of water vapor (P_{H_2O}).

At lower temperature the ambient P_{H_2O} is high enough to result in complete hydration of the apatite phase and this forces the compositions to lie on one of the binary joins $SrO + Sr_{10}(PO_4)_6(OH_2)$ or $Sr_{10}(PO_4)_6(OH)_2 + Sr_3(PO_4)_2$ depending upon the $SrO:P_2O_5$ ratio. In this way the formation of $Sr_4P_2O_9$ is prevented at lower temperatures. As the temperature is increased, the ambient water vapor pressure becomes too low to ensure complete hydration of the apatite phase and the compositions move off the binary joins toward the bounding system $SrO–P_2O_5$. Incompletely dehydrated samples end up in one of the two-phase regions or in the three-phase region $SrO + Sr_4P_2O_9 + Sr_{10}(PO_4)_6(OH)_2$. By following the dehydration path appropriate to each sample, all of the data in Table II can be accounted for, provided that it is recognized that the samples are slightly richer in P_2O_5 than indicated. A very small weighing error would result in considerable contamination of supposedly stoichiometric samples by second phases since the three compounds $Sr_4P_2O_9$, $Sr_{10}(PO_4)_6O$, and $Sr_3(PO_4)_2$ are so similar in terms of weight or molar composition. The samples melting at 1650° appear to be completely dehydrated, but no quantitative proof of this statement can be given.

If strontium oxyapatite did not exist, the hydroxylapatite would dissociate into $Sr_3(PO_4)_2$ and $Sr_4P_2O_9$ when dehydrated at high temperature. As may be seen from Table V this does not occur in the strontium system but does occur in the calcium system. It may therefore be concluded that $Sr_{10}(PO_4)_6O$ exists but that $Ca_{10}(PO_4)_6O$ does not exist. These results are in agreement with the conditions given by Balz[8] for the existence of the oxyapatites. In addition, if oxyapatite did not exist, the diagram would contain the three-phase region [$Sr_4P_2O_9 + Sr_{10}(PO_4)_6(OH)_2 + Sr_3(PO_4)_2$], and this phase assemblage was never observed experimentally.

Comparison with the $CaO–P_2O_5$ System

Attempts to prepare the strontium analogs of $Ca_2P_6O_{17}$ and CaP_4O_{11}[12] were unsuccessful. Both compositions produced glasses when heated at 550°. The $Sr_2P_6O_{17}$ glass was partially devitrified at 490° and gave a mixture of β-$Sr(PO_3)_2$ and glass. This fact indicates that either the compound $Sr_2P_6O_{17}$ does not exist or it has an incongruent melting point below 490°. This part of the $SrO–P_2O_5$ system was not studied in sufficient detail to state unequivocally that $Sr_2P_6O_{17}$ and SrP_4O_{11} do not exist.

TABLE V

THE THERMAL BEHAVIOR OF STRONTIUM AND CALCIUM HYDROXYLAPATITES

Starting phase	Heat treatment, deg/hr	Phases present	Remarks
$Ca_{10}(PO_4)_6(OH)_2$	1300/34	$Ca_{10}(PO_4)_6(OH)_2$	In air
	1360/2	α-$Ca_3(PO_4)_2 + Ca_4P_2O_9$	Vacuum
	1420/2	α-$Ca_3(PO_4)_2 + Ca_4P_2O_9$	In air
	1650/10 sec	α-$Ca_3(PO_4)_2 + Ca_4P_2O_9$	Fused in air, SF
$Sr_{10}(PO_4)_6(OH)_2$	1240/11	$Sr_{10}(PO_4)_6(OH)_2$	In air
	1450/3	$Sr_{10}(PO_4)_6(O,OH)_2$	In air
	1420/2	$Sr_{10}(PO_4)_6O$	Vacuum
	1650/10 sec	$Sr_{10}(PO_4)_6O$	Fused in air, SF

A check of the $CaO–P_2O_5$ system for solid solutions (Table VI) indicated (a) that the orthophosphate solid solutions reported by Welch and Gutt[11] do not exist, (b) that $7CaO{\cdot}5P_2O_5$ is stable at temperatures at least as low as 800° and does not have a lower limit of stability at 920° as reported by Hill, Faust, and Reynolds,[12] and (c) that no peak shifts could be observed in the X-ray pattern for calcium-rich tromelite as a function of temperature as would be predicted by the diagram of Hill, Faust, and Reynolds.[12] The most likely source of error in the work of Welch and Gutt[11] is the loss of P_2O_5 from the system during observation of the melting behavior (<1600°) of samples on the high-temperature microscope stage. This would, for example, cause a mixture of $Ca_2P_2O_7$ and $Ca_3(PO_4)_2$ to shift in total composition toward $Ca_3(PO_4)_2$, and subsequent X-ray analysis would reveal the existence of only $Ca_3(PO_4)_2$. Thus the reported solid solution limit probably represents the extent to which P_2O_5 is lost from the system. In view of the severe vaporization problems which would be encountered above 1700° in air, the temperature maximum in the α-$Ca_3(PO_4)_2$(ss) region is suspect and 1777° could be the congruent melting point of stoichiometric $Ca_3(PO_4)_2$. In the case of Hill, Faust, and Reynolds,[12] it is likely that nonequilibrium affected their study of the $CaO–P_2O_5$ system in the meta–pyro region.

TABLE VI

ACCURATE 2θ MEASUREMENTS ON PHASES IN THE SYSTEM $CaO–P_2O_5$ AS A CHECK FOR SOLID SOLUTIONS

$Ca_2P_2O_7$	$Ca_2P_2O_7 + Ca_3(PO_4)_2$	$Ca_3(PO_4)_2$	
26.91 ± 0.01	26.90 ± 0.01	...	Equilibrated at 1250° for 20 hr
27.73	27.73	...	
28.98	28.99	...	
42.99	43.00	...	
45.64	45.67	...	
...	30.38	30.37 ± 0.01	
...	30.72	30.72	
...	31.29	31.29	
...	34.24	34.23	
...	46.83	46.82	
	$7CaO{\cdot}5P_2O_5 + Ca_2P_2O_7$ at 870°	($7CaO{\cdot}5P_2O_5$ peaks) at 960°	
	39.39 ± 0.01	39.40 ± 0.01	
	45.04	45.05	
	48.80	48.79	

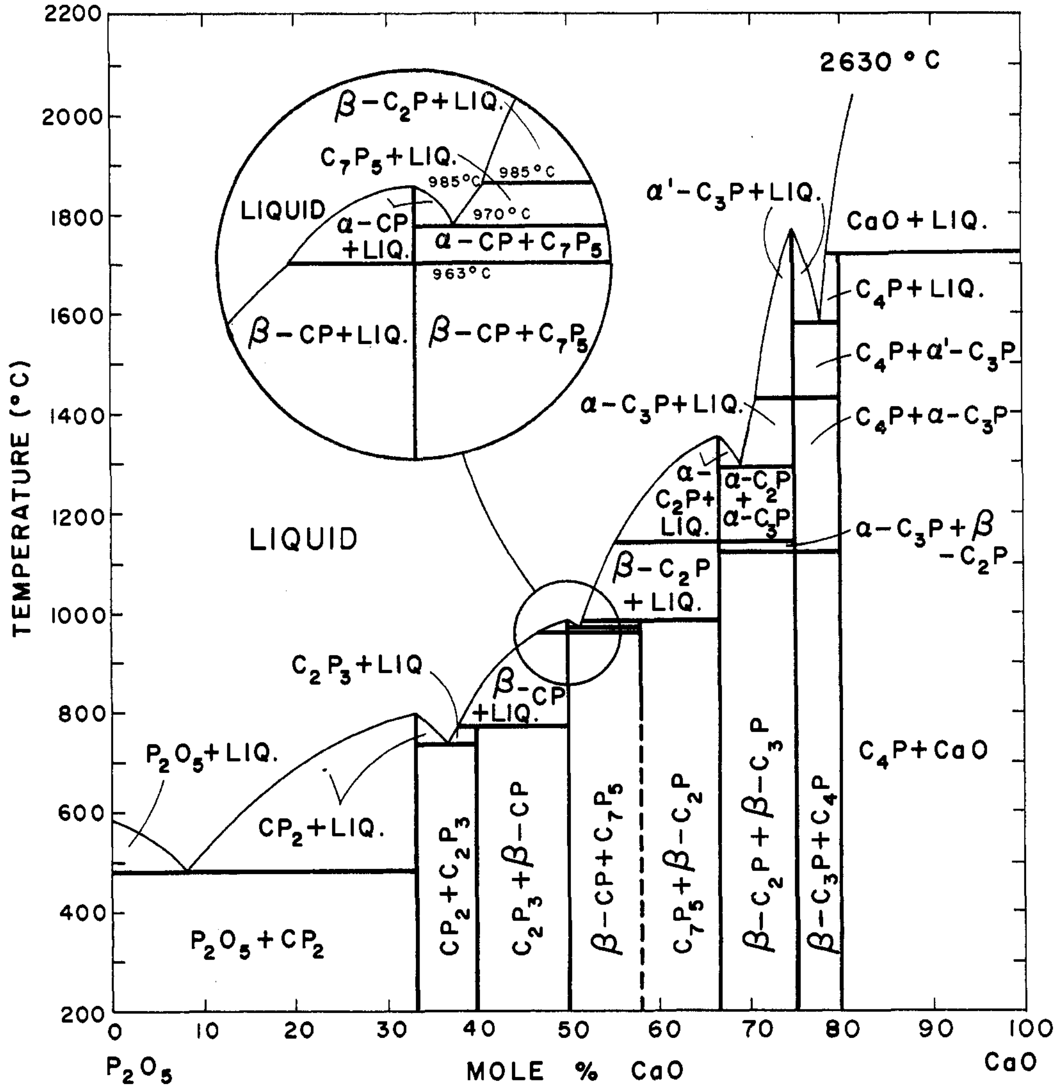

Figure 3.—Tentatively revised equilibrium diagram for the system $CaO-P_2O_5$: C = CaO; P = P_2O_5.

By analogy with the $SrO-P_2O_5$ system, and on the basis of the limited experimental data for the $CaO-P_2O_5$ system, a new diagram for the $CaO-P_2O_5$ system is proposed (Figure 3). The melting points and inversion temperatures were taken from the literature. It is suggested that a careful reinvestigation of the system $CaO-P_2O_5$ is in order and that, while Figure 3 may be generally correct, it should be regarded as tentative. In any case the diagram published by Welch and Gutt is definitely incorrect, and the work of Hill, Faust, and Reynolds is at least partially incorrect. The diagram by Tromel, Harkort, and Hotop[10] appears to be the most dependable of the previously published diagrams.

The analogous compounds in the two systems exhibit the same melting behavior. A visual comparison of X-ray diffraction patterns showed that β-$Ca(PO_3)_2$ and β-$Sr(PO_3)_2$ are isotypic and that β-$Ca_2P_2O_7$ and β-$Sr_2P_2O_7$ are isotypic. In addition, β-$Ca_3(PO_4)_2$ and β-$Sr_3(PO_4)_2$ and $Ca_4P_2O_9$ and $Sr_4P_2O_9$ have been reported to be isotypic.[2,5] There does not appear to be an analog of $Sr_3P_4O_{13}$ in the calcium system. Instead, there is a compound having the composition $7CaO \cdot 5P_2O_5$. No analog of $Sr_{10}(PO_4)_6O$ exists in the calcium system.

Acknowledgment.—The authors are grateful to the Lamp Division of the General Electric Co., Nela Park, Cleveland, Ohio, for the financial support which made this work possible.